

# Investigation of Approaches for the Localization of Anatomical Landmarks in 3D Medical Images

Wolfgang Beil, Karl Rohr, H. Siegfried Stiehl<sup>a\*</sup>

<sup>a</sup>Universität Hamburg, FB Informatik, AB KOGS  
Vogt-Kölln-Str. 30, D-22527 Hamburg, Germany

We investigate the extraction of corresponding anatomical point landmarks in MR and CT images of the human head using 3D differential operators for the extraction of isocontour curvature extrema. We carried out experiments measuring the sensitivity to noise, the localization accuracy, the false detection rate and the registration accuracy. Based on the experimental results we compare the performance of six different approaches.

## 1. Introduction

Several approaches have been proposed in the literature to register images of different modalities on the basis of corresponding anatomical point landmarks e.g. [1], [2], [3]. These point landmarks are usually localized manually which is time consuming and error-prone in clinical routine applications. It is therefore necessary to relieve the physician of this tedious routine work and to improve the accuracy and reproducibility of the localizations. In this paper we present an approach to localize semi-automatically landmarks characterized by extremal isocontour curvature. The semi-automatic approach implies that a rough estimate of the landmark position centered at a volume-of-interest is interactively provided by the user as an input. The algorithm then refines this position [10].

Monga and Benayoun [4] presented an approach to compute locally the curvature characteristics of isosurfaces. The gradient direction is used to define locally the tangent plane of the isosurface. Then a local parametrization is defined by setting up two arbitrary orthogonal vectors within this tangent plane. Given this parametrization they show how the principal curvatures of the isosurface and the associated principal directions can be computed. Additionally, they derive an extremality criterion based on the spatial derivative of the principal curvature in direction of the corresponding principal direction. Application of this extremality criterion in maximum curvature direction yields a 1D subset of points on the isosurface which they call ridge (or crest) lines.

Thirion [6] proposed an algorithm to extract automatically isocontour curvature extrema, which he denoted *extremal points*, from 3D images and which then serve as input for a rigid registration algorithm. His algorithm basically uses the extremality criterion of Monga and Benayoun [4] in both principal curvature directions.

---

\*This work was funded by the Philips Research Laboratories Hamburg, project IMAGINE

We started out from an investigation of anatomical point landmarks presented in the literature [1], [2], [3]. We focused on such landmarks which can be characterized as isocontour curvature extrema and which are localizable in MR as well as in CT data sets.

## 2. Curvature of isocontours

Isosurfaces in 3D images are hyperplanes  $t(r, s)$  of constant intensity:

$$L(r, s, t(r, s)) = L(P) = \text{const} \quad (1)$$

From differential geometry follows that the curvature of a surface in 3D is orientation dependent according to the following equation derived by Euler [9]:

$$t_2(\alpha) = \frac{1}{2}(t_{rr} + t_{ss}) + \frac{\cos(2\alpha)}{2}(t_{rr} - t_{ss}) \quad (2)$$

with  $t_{rr}$  and  $t_{ss}$  being the principal curvatures and  $\alpha$  denoting the orientation in the tangent plane. The corresponding principal curvature directions are vectors in the tangent plane to the surface and equation (2) assumes that these directions equal the  $r$  and  $s$  coordinate axes. By computing implicit derivatives of equation (1), isocontour curvature and the derivative of isocontour curvature can be related to partial derivatives of the image intensity function [7], [11]. The principal curvatures of isosurfaces read:

$$t_{rr} = -\frac{L_{rr}}{L_t} \quad , \quad t_{ss} = -\frac{L_{ss}}{L_t} \quad (3)$$

### 2.1. Extremality criterion

The derivative of isocontour curvature in principal curvature direction is given by:

$$t_{rrr} = \frac{3L_{rt}L_{rr}}{L_t^2} - \frac{L_{rrr}}{L_t} \quad (4)$$

(and analogous for  $t_{sss}$ ). The conditions  $t_{rrr} = 0$  and  $t_{sss} = 0$  define points of extremal curvature on isocontours and can be used to localize anatomical landmarks having this differential geometric characterization. Monga and Benayoun [4], [5] derived this criterion under the assumption that the principal curvature direction is locally constant and obtained:

$$t_{rrr} = \frac{L_{rt}L_{rr}}{L_t^2} - \frac{L_{rrr}}{L_t} \quad (5)$$

For synthetically generated images we observed that an extremality criterion based on this equation yields invalid results for non-symmetrical isocontours w.r.t. the gradient vector at the extremum, i.e.  $L_{rrr} \neq 0$ .

### 2.2. Alternative criteria

Instead of using the derivative of isocontour curvature it is also possible to apply non-maximum-suppression of principal curvature in both principal curvature directions. Monga and Benayoun [4] extracted ridge lines with this alternative criterion.

Another approach is to search for local extrema of mean or Gaussian curvature. The sum and product of both principal curvatures are denoted *mean* and *Gaussian* curvature, respectively [9]:

$$MC = \frac{t_{rr} + t_{ss}}{2} \quad , \quad GC = t_{rr} \cdot t_{ss} \quad (6)$$

Detecting local extrema of mean or Gaussian curvature is computationally less expensive, since they are rotationally invariant and can be determined without computing the principal curvature directions first.

All criteria mentioned so far apply to each isocontour. In order to arrive at point landmarks the approaches based on these criteria first select points with extremal gradient magnitude (via edge detection) and afterwards apply the criteria only to this subset of points. A simple alternative which computes neither edges nor principal curvature directions is to search for local extrema of mean or Gaussian curvature multiplied with some power of the gradient magnitude. In this case the gradient weighting prefers points with high gradient magnitude. The computationally least expensive way is to use the third or fourth power of gradient magnitude in case of mean or Gaussian curvature, respectively.

### 3. Approaches for landmark localization

We have implemented the following six approaches for the localization of isocontour curvature extrema:

- Zero-crossing approach (*ZeroCr*): This approach is a slight modification of the algorithm proposed in [6]. We use the correct extremality criterion (equation (4)) and select edges by computing zero-crossings of the second-order directional derivative in gradient direction.
- Non-maximum-suppression approach (*NonMaxS*): After Canny edge detection [8] non-maximum suppression of both principal curvatures (absolute values) in the corresponding principal curvature directions is performed. This is an extension of the work presented in [4].
- Gaussian curvature on detected Canny edges (*CannyGC*): Locally extremal values of Gaussian curvature on the edge contour are determined.
- Mean curvature on detected Canny edges (*CannyMC*): Locally extremal values of mean curvature on the edge contour are determined.
- Gradient weighted Gaussian curvature approach (*gwGC*): Locally extremal values of Gaussian curvature multiplied with the fourth power of the gradient magnitude are determined.
- Gradient weighted mean curvature approach (*gwMC*): Locally extremal values of mean curvature multiplied with the third power of the gradient magnitude are determined.

All of these algorithms can cope with anisotropic voxel sizes. This is achieved by: i) voxel size dependent smoothing using cubic B-splines for interpolation, ii) voxel size dependent weighting of partial derivatives, and iii) transformation between covariant and contravariant vectors.

#### 4. Experiments

The above approaches were tested on synthetical data as well as on landmarks in MR and CT datasets of four different patients. Our landmark set contained 6 midsagittal and 12 hemispherical 3D landmarks which are: saddle point on top of medulla oblongata; curvature extremum on the anterior surface of cerebellum; top of nasal bone; two curvature extrema on the ridge lines between medulla oblongata and pons; external protuberance and clinoid process; tip of the frontal horn and occipital horn of the lateral ventricles; tip of the temporal horn of the lateral ventricles; saddle points on zygomatic bone; and saddle points on mastoid process.

We compared our approaches on the basis of the following experiments:

- **Noise experiments:** We carried out experiments in order to investigate the sensitivity to noise of the different approaches. Based on volumes-of-interest extracted from a MR image with high signal-to-noise ratio ( $\text{SNR} = 30$ ) and on three synthetically generated ellipsoids representing curvature extrema on different scales, the effects of additional additive Gaussian noise were investigated for each approach. The following SNRs (defined as the ratio of signal contrast and the standard deviation of the added Gaussian noise) were used in the experiments: 16, 8, 4, 2, 1, and 0.5. These values were chosen in order to cover the range of SNRs we found for ventricular structures in the CT volumes of the patient datasets, which varied between 1.6 and 2.5. Gaussian smoothing was varied between  $\sigma = 0.8$  and 3.0 in steps of 0.2. As a result the localized positions of the ZeroCr, NonMaxS, and CannyGC approaches agreed very well. But outliers were present in the localization results of both, the NonMaxS and the CannyGC approaches. It turned out that these outliers were due to the higher noise-sensitivity of the non-maximum-suppression scheme in comparison to the zero-crossing detection scheme. No useful localizations were obtained for  $\text{SNR} = 0.5$ , but for  $\text{SNR} \geq 2$  the observed localization errors were small. The gwGC and gwMC approaches had larger displacements if higher degrees of Gaussian smoothing were used. The localization errors of the CannyMC and the gwMC approaches were significantly higher compared to the other approaches.
- **Localization accuracy:** Positions of the whole landmark set determined with the six approaches in a  $7 \times 7 \times 7$  volume-of-interest were compared in MR and CT data sets of four different patients. We used the ZeroCr approach as a reference for the localizations of the other approaches. It turned out that identical or adjacent voxels were localized by the ZeroCr, the NonMaxS, and the gwGC approaches in 93% of all cases. A significantly higher number of mismatches was observed for the CannyGC approach. As expected from the above noise experiments the localizations of the CannyMC and the gwMC approaches also differed significantly.
- **False detection rate:** For each of the landmarks, for each modality and for each

approach except for the CannyMC and gwMC approaches the number of false detections was plotted vs. the distance to the landmark position obtained previously in the localization experiments. We defined the operator response for each approach as the product of both principal curvatures multiplied with the fourth power of the gradient magnitude. A detection was regarded a false detection if the operator response at this voxel was larger than the operator response at the previously detected landmark position. An example is presented in Fig. 1.

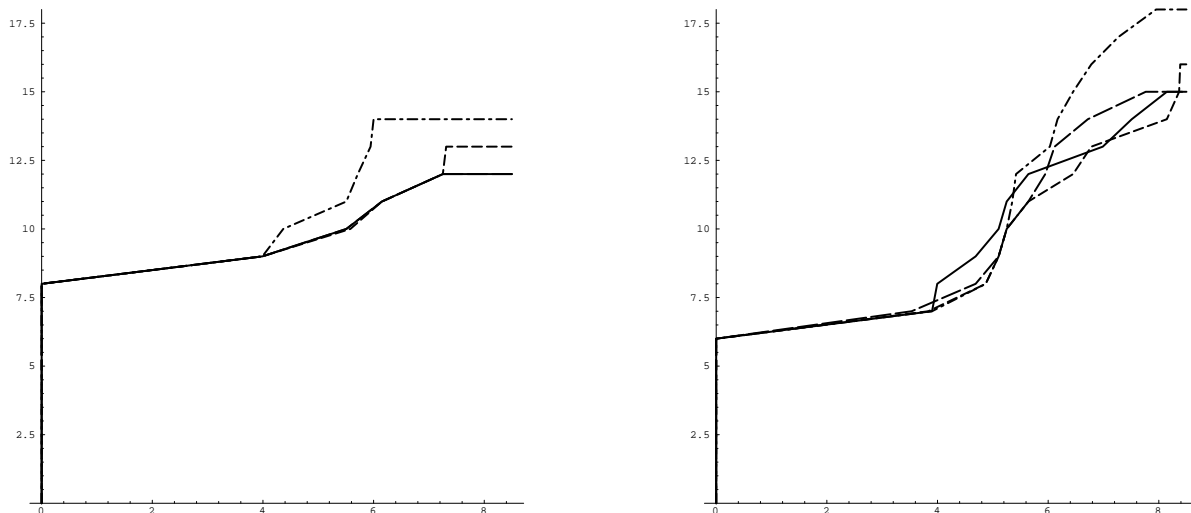


Figure 1. False detections (ordinate) vs.  $mm$ -distance (abscissa) for the tip of the frontal horn localized with ZeroCr (full line), NonMaxS (short dashes), gwGC (long dashes), and CannyGC (dot-dashed line) approaches in MR (left) and CT (right). Note, that the cumulated numbers include the reference detection.

- **Affine registration accuracy:** An affine transformation which minimizes the registration error of the landmarks in a least-squares sense was calculated. The registration errors at the landmarks were compared. It turned out that for most of the landmarks the registration errors were in the range of 1 to 3  $mm$ .

## 5. Conclusion

We first investigated the performance of six different approaches for the extraction of isocontour curvature extrema given several images artificially degraded with different signal-to-noise ratios. The conclusion from these experiments on synthetical data is that the ZeroCr approach slightly outperforms the other approaches since we did not observe outliers for this approach. However, its algorithmic complexity and its computational costs are high. In initial investigations on tomographic data we found that a set of 18 promising landmark candidates seemed to be suited for a further validation of the approaches. Investigating four patient datasets it turned out that the localizations obtained with the NonMaxS and the gwGC approaches agreed very well with those of the ZeroCr approach. The larger displacements of the gwGC approach did not pose a practical

problem since they occurred only for large amounts of smoothing ( $\sigma \geq 1.6$ ) and did not affect the affine registration accuracy. The localization performance of the CannyMC and gwMC approaches were significantly worse compared to the other approaches.

In the experiments w.r.t. the false detection rate as defined above it was possible to reliably localize the set of landmarks in the MR and CT data sets within a landmark-centered radius of  $5\text{ mm}$ . But we found significant differences regarding the false detection rate for the different landmarks. Especially the landmarks 'external protuberance', 'saddle point on zygomatic bone', and 'occipital horn of the lateral ventricle' had low false detection rates. The measurements of the registration accuracy confirmed our findings w.r.t. the localization accuracy. Except for landmark 'top of nasal bone' the affine registration errors at the landmarks were below  $4\text{ mm}$ .

## REFERENCES

1. A.C. Evans, W. Dai, L. Collins, P. Neelin, and S. Marrett, (1991) Warping of a computerized 3-D atlas to match brain image volumes for quantitative neuroanatomical and functional analysis. Medical Imaging V: Image Processing, San Jose, California/USA, Proc. SPIE 1445, M.H. Loew (Ed.), 236 - 246
2. D.L.G. Hill, D.J. Hawkes, J.E. Crossman, M.J. Gleeson, T.C.S. Cox, E.E.C.M. Bracey, A.J. Strong, and P.Graves (1991) Registration of MR and CT images for skull base surgery using point-like anatomical features. The British Jour. of Radiology 64(767), 1030 - 1035
3. F.L. Bookstein (1989) Principal Warps: Thin-Plate Splines and the Decomposition of Deformations. IEEE Trans. on Pattern Analysis and Machine Intelligence (PAMI) 11(6), 567 - 585
4. O. Monga and S. Benayoun (1995) Using partial derivatives of 3D images to extract surface features. Comp. Vision and Image Underst. 61(2), 171 - 189
5. O. Monga, S. Benayoun, and O.D. Faugeras (1992) From partial derivatives of 3D density images to ridge lines. Proc. of CVPR92, Urbana Champaign, Illinois, pp. 354 - 359
6. J-P. Thirion (1994) Extremal points: definition and application to 3D image registration. Proc. of CVPR94, 587 - 592
7. J.P. Thirion and A. Gourdon (1995) Computing the Differential Characteristics of Isointensity Surfaces. Comp. Vision. and Image Underst. 61(2), 190 - 202
8. J. Canny (1986) A computational approach to edge detection. IEEE Transactions on Pattern Analysis and Machine Intelligence 8(6), 679 - 698
9. J.J. Koenderink (1990). Solid shape. The MIT Press, Cambridge MA
10. K. Rohr, H.S. Stiehl, R. Sprengel, W. Beil, T.M. Buzug, J. Weese, and M.H. Kuhn (1996) Point-Based Elastic Registration of Medical Image Data Using Approximating Thin-Plate Splines. Proc. 4th Int. Conf. Visualization in Biomedical Computing (VBC96), Hamburg, Germany, Lecture Notes in Computer Science 1131, K.H. Höhne and R. Kikinis (Eds.), Springer, 297 - 306
11. L.M.J. Florack, B.M. ter Haar Romeny, J.J. Koenderink, M.A. Viergever (1992) Scale and the differential structure of images. Image and Vision Computing 10, 376 - 388